

Cooperative non-equilibrium phase transition in a dilute thermal atomic gas

C. Carr, R. Ritter, C. S. Adams, and K. J. Weatherill
Joint Quantum Centre (JQC) Durham-Newcastle, Department of Physics,
Durham University, South Road, Durham, DH1 3LE, United Kingdom
(Dated: March 29, 2013)

We demonstrate a non-equilibrium phase transition in a dilute thermal atomic gas. The phase transition is induced by dipole-dipole interactions between Rydberg atoms which are separated by less than the transition wavelength to neighbouring states. In the frequency domain we observe a cooperative shift of the Rydberg state which results in intrinsic optical bistability above a critical number of excited atoms. In the time domain we observe critical slowing down where the correlation length diverges with critical exponent $\alpha = -0.53 \pm 0.10$. The atomic emission spectrum in the many-body phase provides strong evidence for a superradiant cascade.

Non-equilibrium systems are found throughout nature, for example in ecosystems, financial markets and climate [1]. The steady-state of a non-equilibrium system is a dynamical equilibrium between driving and dissipative processes. As a result, the complex dynamics cannot be described within the well-established framework of equilibrium thermodynamics. Phase transitions in non-equilibrium systems are particularly interesting as they are a consequence of macroscopic long-range correlation in a system with microscopic interactions [2]. Whilst the theoretical analysis of dynamical phase transitions has provided much insight [3–6], experimental work is still in its infancy. Recent work has detailed the emergence of spatial structures in a cold atomic gas [7] and dissipation-induced correlation in a cold molecular gas [8]. Here we demonstrate a non-equilibrium phase transition [9] in a dilute optically-driven thermal gas.

The long-range correlation in our non-equilibrium system arises due to cooperative dipole-dipole interactions between atoms. The level of cooperativity can be quantified through the cooperativity parameter $\mathcal{C} = \mathcal{N}\lambda^3/4\pi^2$, defined by the atomic number density \mathcal{N} and the transition wavelength λ . When the number of atoms per cubic transition wavelength is large ($\mathcal{C} \gg 1$), phenomena such as superradiance [10–13] and level shifts [13, 14] become important. For ground state atoms, the study of cooperative effects is usually limited to dense media [14], solid-state systems [13] and Bose gases confined to cavities [15]. Here we are able to access the cooperative regime in a dilute gas by performing narrowband laser excitation to highly-excited Rydberg states [16, 17] where the dipole-dipole interaction [18–21] and optical non-linearity [22–28] are many orders of magnitude larger. The fact that the transition wavelength to neighbouring Rydberg states is of the order of 1 mm enables us to observe a non-equilibrium phase transition on macroscopic, optically-resolvable length scales.

The direct observation of a cooperative non-equilibrium phase transition is illustrated schematically in Fig. 1. The experiment, shown in Fig. 1(a), consists of a thermal vapour of caesium atoms confined in a quartz

cell with an optical path length of 2 mm [29]. The atoms are driven into the $26p_{3/2}$ Rydberg state using three excitation lasers which co-propagate through the cell [30]. The probe laser, with wavelength $\lambda_P = 852.3$ nm and Rabi frequency Ω_P , is resonant between the ground state $6s_{1/2}$ and the excited state $6p_{3/2}$. The laser is fre-

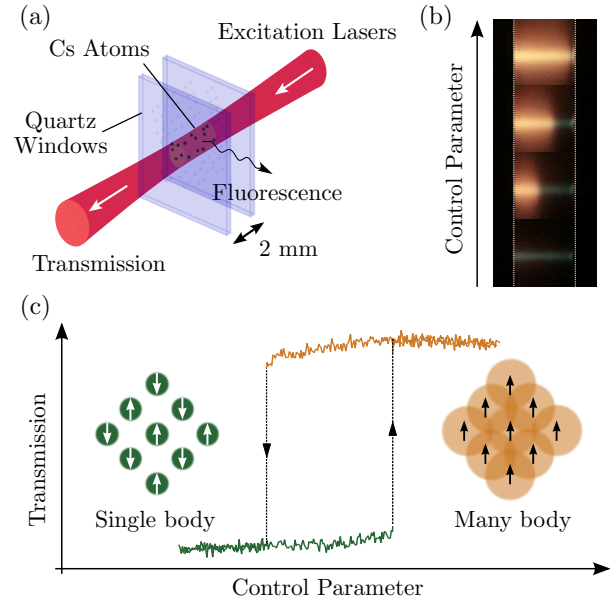


FIG. 1. (color online) Observation of a cooperative non-equilibrium phase transition. (a) The excitation lasers co-propagate through a 2 mm cell of caesium vapour. The first-order phase transition is exhibited as (b) an abrupt switch in the off-axis fluorescence and (c) intrinsic optical bistability in the probe laser transmission. At a critical control parameter the system discontinuously jumps between single-body (green / dark grey) and many-body (orange / light grey) behaviour. Experimental parameters: ground state density $\rho_G = 4.3 \times 10^{12} \text{ cm}^{-3}$, probe Rabi frequency $\Omega_P = 2\pi \times 110$ MHz, coupling Rabi frequency $\Omega_C = 2\pi \times 200$ MHz and Rydberg Rabi frequency $\Omega_R = 2\pi \times 330$ MHz. The control parameter, in this case the Rydberg laser detuning, is varied around $\Delta_R = 2\pi \times -220$ MHz. The dashed white lines in (b) indicate the 2 mm optical path length.

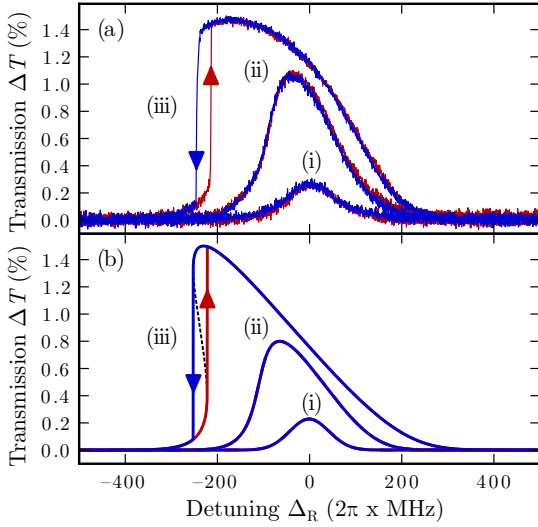


FIG. 2. (color online) Intrinsic optical bistability in the optical response of the ensemble. (a) Experimental and (b) theoretical optical response ΔT as a function of Rydberg laser detuning Δ_R for Rydberg Rabi frequency Ω_R increasing from (i) to (iii). Experimental parameters: ground state density $\rho_G = 4.3 \times 10^{12} \text{ cm}^{-3}$, probe Rabi frequency $\Omega_P = 2\pi \times 100 \text{ MHz}$, coupling Rabi frequency $\Omega_C = 2\pi \times 220 \text{ MHz}$ and Rydberg Rabi frequency $\Omega_R = 2\pi \times (30, 80, 160) \text{ MHz}$. Theoretical parameters: cooperative shift $S = 2\pi \times (0.81, 153) \text{ MHz}/\Delta T$ and Gaussian width $\sigma = 2\pi \times (60, 100, 140) \text{ MHz}$.

quency stabilised to the $|6s_{1/2}, F=4\rangle \rightarrow |6p_{3/2}, F'=5\rangle$ transition. The coupling laser, with wavelength $\lambda_C = 1469.9 \text{ nm}$ and Rabi frequency Ω_C , is resonant between the excited states $6p_{3/2}$ and $7s_{1/2}$. Using excited state polarisation spectroscopy [31], the laser is stabilised to the $|6p_{3/2}, F'=5\rangle \rightarrow |7s_{1/2}, F''=4\rangle$ transition. Finally the Rydberg laser with wavelength $\lambda_R = 790.3 \text{ nm}$ and Rabi frequency Ω_R , is tuned around the resonance between the excited-state $7s_{1/2}$ and the Rydberg state $26p_{3/2}$.

When the number of Rydberg atoms is small ($C \ll 1$), the system exists in a few-body disordered state and the induced Rydberg dipoles oscillate with a random phase. At a critical Rydberg number density, the entire medium undergoes a phase transition to a many-body ordered state ($C \gg 1$) where the dipoles oscillate in-phase. In our experiment, the control parameter is the number of Rydberg atoms in the ensemble and this is determined by the ground state number density ρ_G , and the intensity I_R and detuning Δ_R of the third-step Rydberg laser.

The phase transition is observed as a dramatic change in the off-axis fluorescence, as shown in Fig. 1(b), clearly visible with the naked eye. This longitudinal phase transition along the beam axis has been predicted theoretically [32] but not previously observed. The phase transition can also be observed as a sudden change in the optical transmission ΔT , as shown in Fig. 1(c). Through

electron shelving [33], the change in probe laser transmission provides a direct readout of the Rydberg population. The conditions for switching between low and high levels of Rydberg excitation depend on the history of the ensemble giving rise to hysteresis and hence optical bistability.

Bistable phenomena occur due to the presence of feedback in a non-linear system [34]. Optical bistability was first observed by placing a non-linear medium in a Fabry-Perot interferometer where the cavity mirrors provide feedback [35]. In the case of intrinsic optical bistability, which we observe here, the feedback originates from the atoms themselves [36]. In the cooperative regime, many atoms are present within a transition wavelength and are therefore coupled by the same dipolar field. The resultant cooperative shift is excitation dependent and leads to an effective frequency renormalisation of the resonance condition [37]. At a critical level of excitation this cooperative shift results in intrinsic optical bistability [38].

The onset of intrinsic optical bistability is shown as a function of Rydberg laser detuning Δ_R for increasing

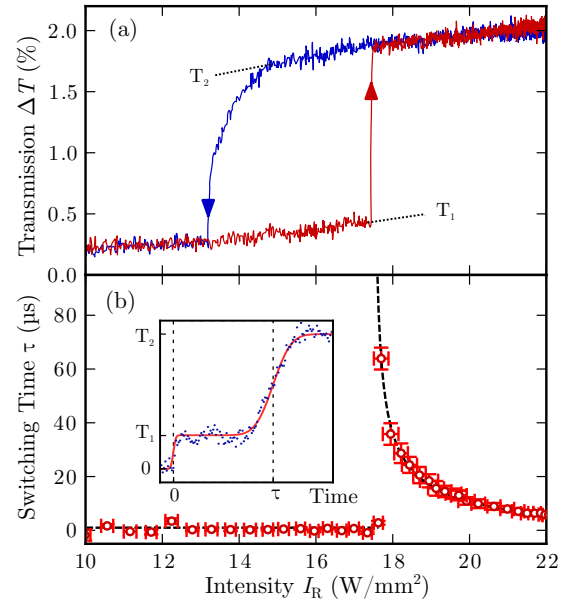


FIG. 3. (color online) Critical slowing down as the temporal signature of a phase transition. (a) Continuous Rydberg laser intensity I_R scan showing bistability and hysteresis in the optical response ΔT . (b) Discrete Rydberg laser intensity I_R scan showing the divergence of the switching time to steady-state τ around the critical transition intensity $I_{R,\text{crit}} \approx 17.5 \text{ W/mm}^2$. The switching time diverges as $(I_R - I_{R,\text{crit}})^\alpha$ with critical exponent $\alpha = -0.53 \pm 0.10$ (standard deviation error) shown by the dashed line of best fit. Ground state density $\rho_G = 4.3 \times 10^{12} \text{ cm}^{-3}$, probe Rabi frequency $\Omega_P = 2\pi \times 150 \text{ MHz}$, coupling Rabi frequency $\Omega_C = 2\pi \times 340 \text{ MHz}$ and Rydberg detuning $\Delta_R = 2\pi \times -220 \text{ MHz}$. The error bars represent the standard deviation error on the determination of the laser intensity and switching time.

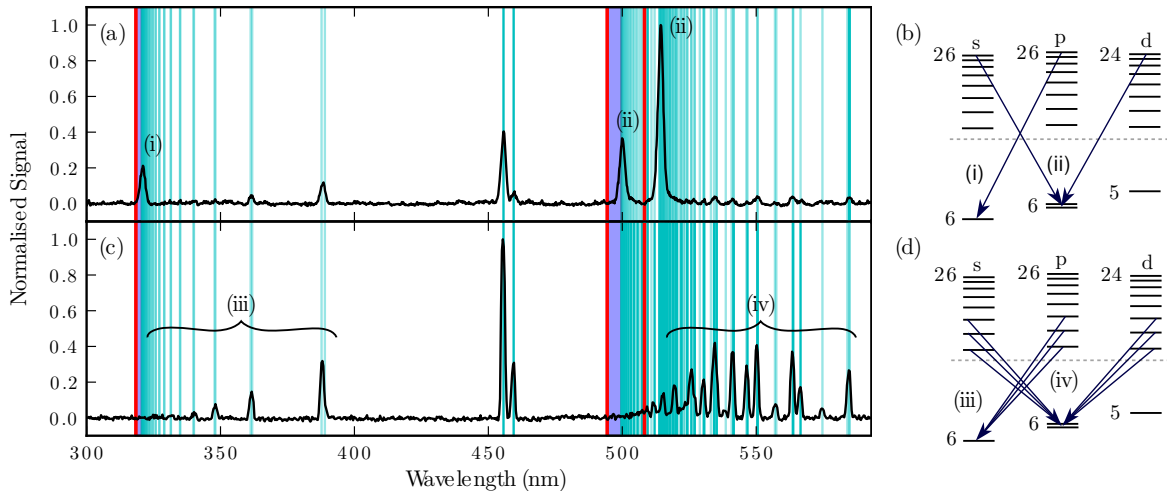


FIG. 4. (color online) Atomic emission spectra in the single-body and many-body phase. The visible fluorescence spectrum is shown for (a) $\rho_G = 3.1 \times 10^{11} \text{ cm}^{-3}$ and (c) $\rho_G = 4.3 \times 10^{12} \text{ cm}^{-3}$. In the single-body phase, the spontaneous emission originates from high-lying Rydberg states as illustrated in (b). However, in the many-body cooperative phase, the spontaneous emission originates from low-lying Rydberg states, as illustrated in (d), due to a superradiant cascade between high-lying Rydberg states. The ionisation limits from $6s_{1/2}$, $6p_{1/2}$ and $6p_{3/2}$ are shown by thick red vertical lines. The blue shaded regions highlight the absence of spontaneous emission between $26p_{3/2}$ and ionisation which would occur due to a blackbody or collisional excitation process. The thin cyan vertical lines indicate the dipole-allowed transitions. Probe Rabi frequency $\Omega_P = 2\pi \times 110 \text{ MHz}$, coupling Rabi frequency $\Omega_C = 2\pi \times 200 \text{ MHz}$ and Rydberg Rabi frequency $\Omega_R = 2\pi \times 330 \text{ MHz}$.

Rydberg Rabi frequency Ω_R in Fig. 2(a). The Rabi frequency provides a measure of the coupling strength to the Rydberg state and is determined by the transition dipole moment and the laser intensity I_R . At low Rydberg Rabi frequency, and therefore low Rydberg population, there is a symmetric increase in probe transmission ΔT around resonance at $\Delta_R = 0$. At moderate Rydberg Rabi frequency (ii), the lineshape becomes asymmetric and shifted to lower frequencies, similar to the cooperative Lamb shift [14]. Finally with high Rydberg Rabi frequency (iii), the lineshape becomes bistable, with a sharp switch between low and high Rydberg population. This bistable behaviour is accompanied by hysteresis which is dependent upon the direction from which resonance is approached (blue (dark grey) curve from higher frequencies and red (light grey) curve from lower frequencies). Importantly, this bistability is measured in steady-state and is not a transient phenomena. As a result, within the hysteresis window the system can be placed in either a single-body or many-body phase for exactly the same experimental parameters.

A simple theoretical model using an excitation-dependent shift is shown in Fig. 2(b). The single-body symmetrical response in Fig. 2(b)(i) is modelled by a Gaussian curve. The asymmetry, bistability and hysteresis in the cooperative many-body response in Fig. 2(b)(ii-iii) is reproduced by the renormalisation $\Delta_R \rightarrow \Delta_R - S \Delta T$ where S is directly proportional to the cooperativity parameter.

The phase transition can be confirmed through the observation of critical slowing down. This temporal signature of a phase transition occurs as the system approaches a critical point and becomes increasingly slow at recovering from perturbations [39, 40]. In Fig. 3(a), the Rydberg laser intensity I_R is varied continuously and the phase transition from single-body to many-body dynamics occurs at critical intensity $I_{R,\text{crit}} \approx 17.5 \text{ W/mm}^2$. The temporal response of the ensemble is measured by discretely varying the Rydberg laser intensity I_R and measuring the time τ to reach steady-state, as illustrated in the inset of Fig. 3(b). At the critical transition, the switching time diverges according to the power law $\tau \propto (I_R - I_{R,\text{crit}})^\alpha$ shown by the fitted dashed line. The critical exponent $\alpha = -0.53 \pm 0.10$ (standard deviation error) is consistent with previous work on first-order phase transitions and optical bistability [41, 42].

The atomic dynamics across the phase transition can be further understood by measuring the visible spectrum of the off-axis fluorescence shown in Fig. 1(b). The emission spectra for the single- and many-body phases are shown in Fig. 4(a) and (c), respectively. In the single-body phase, the dominant transitions indicated by (i) and (ii) involve decay from high-lying Rydberg states to the ground states of the s, p and d series. This behaviour, highlighted in Fig. 4(b), is consistent with spontaneous emission where such transitions dominate due to the ω^3 dependence in the Einstein A-coefficient.

In the many-body cooperative phase the emission spec-

trum is dramatically modified. The dominant spontaneous emission transitions (i) and (ii) are no longer present. Instead, the spontaneous emission now originates from a range of low-lying Rydberg states indicated by (iii) and (iv) and highlighted in Fig. 4(d). Furthermore, the absence of emission in the blue shaded regions indicates that atoms have not been promoted to higher-lying Rydberg states, as would occur in a collisional process. We can also neglect the effects of thermal black-body photons because the average number of photons per mode at Rydberg-Rydberg transition frequencies is much lower than the average number of excited atoms [12]. The transitions at 455 nm and 459 nm occur in both phases and correspond to decay to $6s_{1/2}$ from $7p_{3/2}$ and $7p_{1/2}$ respectively.

The emission spectrum in the many-body phase can be understood as a superradiant cascade to lower-lying Rydberg states [43]. Evidence for a superradiant cascade has also been observed in ultracold atoms [44, 45]. When the cooperativity on a particular transition is high, the atoms emit collectively and in-phase with one another. Within the excitation volume, we estimate a Rydberg atom number $N_R \approx 1 \times 10^6$ [29] and a single-atom spontaneous lifetime $\tau \approx 500 \mu\text{s}$ on the $26p_{3/2}$ to $26s_{1/2}$ transition. We therefore expect that the superradiant decay occurs on a timescale $\tau_{\text{super}} = \tau/N_R \approx 500$ ps. This is much faster than the spontaneous transitions indicated by (i) and (ii) where $\tau \approx 20 \mu\text{s}$. As the cooperativity parameter $C \propto n^3$, where n is the principal quantum number, the superradiant cascade eventually stops and gives rise to the observed spontaneous emission from low-lying Rydberg states as indicated in Fig. 4(iii) and (iv).

In summary, we have demonstrated a cooperative non-equilibrium phase transition in a dilute thermal atomic gas. The observations that have been discussed raise interesting possibilities for future non-local propagation experiments which utilise the long range cooperative interaction [46]. Furthermore, this work could be used to perform precision sensing [47] around the critical point and to study resonant energy transfer [48] on optically-resolvable length scales. In addition, studies of the fluorescence in the vicinity of the phase transition could provide further insight into the dynamics of strongly-interacting dissipative quantum systems [3, 4].

We would like to thank S A Gardiner and U M Krohn for stimulating discussions, R Sharples for the loan of equipment and M P A Jones and I G Hughes for proof-reading the manuscript. We acknowledge financial support from EPSRC and Durham University.

-
- [1] H. Haken, *Naturwissenschaften* **67**, 121 (1980).
 [2] H. Hinrichsen, *Adv. Phys.* **49**, 815 (2000).

- [3] T. E. Lee, H. Häffner, and M. C. Cross, *Phys. Rev. Lett.* **108**, 023602 (2012).
 [4] C. Ates, B. Olmos, J. P. Garrahan, and I. Lesanovsky, *Phys. Rev. A* **85**, 043620 (2012).
 [5] S. Diehl, A. Tomadin, A. Micheli, R. Fazio, and P. Zoller, *Phys. Rev. Lett.* **105**, 015702 (2010).
 [6] E. M. Kessler, G. Giedke, A. Imamoglu, S. F. Yelin, M. D. Lukin, and J. I. Cirac, *Phys. Rev. A* **86**, 012116 (2012).
 [7] P. Schauß, M. Cheneau, M. Endres, T. Fukuhara, S. Hild, A. Omran, T. Pohl, C. Gross, S. Kuhr, and I. Bloch, *Nature Photon.* **491**, 87 (2012).
 [8] N. Syassen, D. M. Bauer, M. Lettner, T. Volz, D. Dietze, J. J. Garcia-Ripoll, J. I. Cirac, G. Rempe, and S. Durr, *Science* **320**, 1329 (2008).
 [9] D. F. Walls, P. D. Drummond, S. S. Hassain, and H. J. Carmichael, *Supplement of the Progress of Theoretical Physics* **64**, 307 (1978).
 [10] R. Dicke, *Phys. Rev.* **93**, 99 (1954).
 [11] N. Rehler and J. Eberly, *Phys. Rev. A* **3**, 1735 (1971).
 [12] J. M. Raimond, P. Goy, M. Gross, C. Fabre, and S. Haroche, *Phys. Rev. Lett.* **49**, 1924 (1982).
 [13] R. Rohlsberger, K. Schlage, B. Sahoo, S. Couet, and R. Ruffer, *Science* **328**, 1248 (2010).
 [14] J. Keaveney, A. Sargsyan, U. Krohn, I. G. Hughes, D. Sarkisyan, and C. S. Adams, *Phys. Rev. Lett.* **108**, 173601 (2012).
 [15] T. Donner, S. Ritter, T. Bourdel, A. Ottl, M. Kohl, and T. Esslinger, *Science* **315**, 1556 (2007).
 [16] A. K. Mohapatra, T. R. Jackson, and C. S. Adams, *Phys. Rev. Lett.* **98**, 113003 (2007).
 [17] H. Kübler, J. P. Shaffer, T. Baluktsian, R. Low, and T. Pfau, *Nature Photon.* **4**, 112 (2010).
 [18] I. Mourachko, D. Comparat, F. de Tomasi, A. Fioretti, P. Nosbaum, V. M. Akulin, and P. Pillet, *Phys. Rev. Lett.* **80**, 253 (1998).
 [19] T. F. Gallagher, *Rydberg Atoms* (Cambridge University Press, 2005).
 [20] H. Schempp, G. Günter, C. S. Hofmann, C. Giese, S. D. Saliba, B. D. DePaola, T. Amthor, M. Weidemüller, S. Sevincli, and T. Pohl, *Phys. Rev. Lett.* **104**, 173602 (2010).
 [21] T. Baluktsian, B. Huber, R. Löw, and T. Pfau, *Phys. Rev. Lett.* **110**, 123001 (2013).
 [22] A. K. Mohapatra, M. G. Bason, B. Butscher, K. J. Weatherill, and C. S. Adams, *Nature Phys.* **4**, 890 (2008).
 [23] J. D. Pritchard, D. Maxwell, A. Gauguier, K. J. Weatherill, M. P. A. Jones, and C. S. Adams, *Phys. Rev. Lett.* **105**, 193603 (2010).
 [24] Y. O. Dudin and A. Kuzmich, *Science* **336**, 887 (2012).
 [25] V. Parigi, E. Bimbard, J. Stanojevic, A. J. Hilliard, F. Nogrette, R. Tualle-Brouri, A. Ourjoumtsev, and P. Grangier, *Phys. Rev. Lett.* **109**, 233602 (2012).
 [26] T. Peyronel, O. Firstenberg, Q.-Y. Liang, S. Hofferberth, A. V. Gorshkov, T. Pohl, M. D. Lukin, and V. Vuletić, *Nature* **488**, 57 (2012).
 [27] D. Maxwell, D. J. Szwer, D. Paredes-Barato, H. Busche, J. D. Pritchard, A. Gauguier, K. J. Weatherill, M. P. A. Jones, and C. S. Adams, *Phys. Rev. Lett.* **110**, 103001 (2013).
 [28] J. D. Pritchard, K. J. Weatherill, and C. S. Adams, in *Annual review of cold atoms and molecules*, Vol. 1, edited by K. Madison, Y. Wang, A. M. Rey, and K. Bongs (World Scientific, 2013) p. 301.

- [29] “See supplementary material,”.
- [30] C. Carr, M. Tanasittikosol, A. Sargsyan, D. Sarkisyan, C. S. Adams, and K. J. Weatherill, *Opt. Lett.* **37**, 3858 (2012).
- [31] C. Carr, C. S. Adams, and K. J. Weatherill, *Opt. Lett.* **37**, 118 (2012).
- [32] Y. Ben-Aryeh, C. M. Bowden, and J. Englund, *Opt. Commun.* **461**, 53 (1987).
- [33] P. Thoumany, T. Germann, T. Hänsch, G. Stania, L. Urbonas, and T. Becker, *J. Mod. Opt.* **56**, 2055 (2009).
- [34] O. Guillot-Noël, L. Binet, and D. Gourier, *Phys. Rev. B* **65**, 245101 (2002).
- [35] H. M. Gibbs, S. L. McCall, and T. N. C. Venkatesan, *Phys. Rev. Lett.* **36**, 1135 (1976).
- [36] C. M. Bowden and C. C. Sung, *Phys. Rev. A* **19**, 2392 (1979).
- [37] O. Guillot-Noël, P. Goldner, and D. Gourier, *Phys. Rev. A* **66**, 063813 (2002).
- [38] M. P. Hehlen, H. U. Gudel, Q. Shu, J. Rai, S. Rai, and S. C. Rand, *Phys. Rev. Lett.* **73**, 1103 (1994).
- [39] R. Bonifacio and P. Meystre, *Opt. Commun.* **29**, 131 (1979).
- [40] M. Scheffer, J. Bascompte, W. A. Brock, V. Brovkin, S. R. Carpenter, V. Dakos, H. Held, E. H. van Nes, M. Rietkerk, and G. Sugihara, *Nature* **461**, 53 (2009).
- [41] G. Grynberg and S. Cribier, *J. Phys. Lett.* **44**, 449 (1983).
- [42] P. C. Hohenberg and B. I. Halperin, *Rev. Mod. Phys.* **49**, 435 (1977).
- [43] F. Gounand, H. Hugon, P. R. Fournier, and J. Berlande, *J. Phys. B* **12**, 547 (2001).
- [44] T. Wang, S. F. Yelin, R. Cote, E. E. Eyler, S. M. Farooqi, P. L. Gould, M. Kostrun, D. Tong, and D. Vrinceanu, *Phys. Rev. A* **75**, 033802 (2007).
- [45] K. J. Weatherill, J. D. Pritchard, R. P. Abel, M. G. Bason, A. K. Mohaptra, and A. C. S, *J. Phys. B: At. Mol. Opt. Phys.* **41**, 2001002 (2008).
- [46] S. Sevinçli, N. Henkel, C. Ates, and T. Pohl, *Phys. Rev. Lett.* **107**, 153001 (2011).
- [47] R. P. Abel, C. Carr, U. Krohn, and C. S. Adams, *Phys. Rev. A* **84**, 023408 (2011).
- [48] M. Sarovar, A. Ishizaki, G. R. Fleming, and K. B. Whaley, *Nature Phys.* **6**, 462 (2010).